Journal of Engineering Science and Technology
Vol. 19, No. 2 (2024) 405 - 423

ENHANCEMENT IN REMOVAL OF CHROMIUM AND LEAD FROM TANNING PROCESS EFFLUENT BY NOVEL ROTATING DISK MESH ELECTRODE AS ANODE FOR ELECTROCOAGULATION: ISOTHERM AND KINETIC STUDIES

ARSHAD IQBAL*, KHADIJA QURESHI,
IMRAN NAZIR UNAR, ZULFIQAR ALI BHATTI1

Chemical Engineering Department, Mehran University
of Engineering and Technology, Jamshoro, Pakistan
*Corresponding Author: engineerarshade@yahoo.com

Abstract

The aim of the study was to investigate enhancement in removal efficiency of chromium (Cr) and lead (Pb) from leather tannery effluent using novel rotating disk mesh electrode with minimal passivation and metal oxide layer on the surface of electrode. The maximum removal efficiencies were as follows chromium (Cr)= 96 % and lead (Pb)= 98.8% achieved under operating conditions of current density 19.73 mA/cm^2,pH=7, RPM=160 and treatment time=90 min obtained with Rotating Disk Mesh Electrode (RDME) as anode for electrocoagulation. RDME was proved to be more efficient than conventional Non-Rotating Disk Electrode (NRDE) and Rotating Disk Electrode (RDE) as anode for electrocoagulation. Surface analysis of anode before and after experiment was conducted using scanning electron microscopy (SEM) and energy dispersive X-Ray Spectrometry (EDX). Inductively coupled plasma (ICP) was used for analysis of Cr and Pb in tannery effluent before and after experiment. SEM analysis shows there is less passivation and metal oxide layer on surface of RDME compared with NRDE and RDE design for electrocoagulation. EDX analysis revealed weight percentage of element on surface of RDME as 10.45% oxygen, 0.31% Cr and 13.74 % Pb; NRDE shows presence of 17.7 % oxygen, 1.90 % Cr and 15.10 % Pb; RDE shows elemental weight percentage of 16.81 % oxygen, 1.51 % Cr and 14.03 % Pb after electrocoagulation process. It has been deducted from EDX analysis that RDME has lesser metal oxide layer on surface of electrode. The Langmuir and Freundlich adsorption isotherm models were used for isotherm studies, and pseudo first order, pseudo second order and intra particular diffusion model was used for kinetic study. The results revealed that Langmuir adsorption isotherm model fit experimental results well, and pseudo order kinetic model fit for kinetic studies to data. Furthermore, the results proven novel RDME design as an electrode design, having great potential for efficient electrode use for treatment when compared to conventional electrodes.

Keywords: Nonrotating disk electrode, Passivation and specific energy consumption, Rotating disk electrode.

1. Introduction

Chromium (Cr) and lead (Pb) are two common heavy metals that are present in various compounds used in tanneries and discharged into bodies of water without sufficient treatment. Wastewater from different stages of tanning contains high concentration of organic and inorganic substances causing pollution. The organic and inorganic chemical used in hides processing to leather do not attach completely with leather due to low efficiency of tanning process. This is fact that leather industry wastewater is mixtures of various substances such as proteins, lipids, sulphur, sulphate, chlorine, dyes, surfactants, natural tannin at high concentrations. These pollutants have the potential to have a significant negative impact on the environment, including air pollution, agriculture contamination, drinking water contamination, marine life danger, and health problems like cancer and neurological disorders [1].

Although it is challenging to treat this wastewater, various approaches have been utilised in the past, including chemical precipitation [2], adsorption [3], micro-emulsion, membrane separation, and biological process [4].The treatment of this wastewater is difficult to achieve using conventional technologies. Conventional processes are expensive and may lead to secondary pollution.

Electrochemical technologies are now used to clean wastewater that has a complicated nature. The advantages of electrocoagulation, such as its simplicity, dependability, cost-effectiveness, low sludge volume, ease of maintenance, and environmental friendliness, have made this technology one of the most effective electrochemical processes [5] and it has drawn interest for treating the wastewater from leather tanneries [6]. Although passivation and the formation of metal oxide layers on electrode surfaces are some of the limitations of electrocoagulation technology.

The author's main goal was to reduce these issues using a novel anode electrode design for the electrocoagulation process and to enable a better selection of anode electrode design for large-scale application. It has been determined from literature different designs of electrode used as anode made from different materials for electrocoagulation process but most of researcher has not focussed on treatment of tannery effluent using RDME for electrocoagulation process.

The goal of this study was to use a novel RDME as an anode in the electrocoagulation process to treat leather tannery effluent, enhancing the effectiveness of chromium and lead removal while requiring less specific energy consumption and producing less harmful sludge. The current study examines the performance of removal and specific energy consumption of RDME design as anode and compare with classical static electrodes as anode.

SEM and EDX were the instrumental techniques used to investigate the electrode's performance through observing passivation and metal oxide layer on surface of various electrodes physically and chemically. ICP was used to determine the chromium and lead in tannery effluent before and after the experiment. The removal performance of chromium and lead data was validated by renowned Langmuir and Freundlich adsorption isotherm models and correlation coefficient (R^2) was used to see the relevance of model with experimental data. To study kinetics pseudo first order, pseudo second order and intra particle diffusion model were used.

2. Material and Methods

2.1. Characterization and Collection of samples

The effluent sample was collected from combined channel for drainage of effluent of various tanneries from Korangi industrial area Karachi Pakistan. The effluent was collected in polyethylene bottle, and it was added with two to three drops of nitric acid (HNO_3) for preservation of sample and stored in refrigerator at a temperature 4 ˚C. The sample was analysed for Cr and Pb using ICP. pH and electrical conductivity (EC) by PHS-3BW Microprocessor pH/mV/Temperature meter. Biochemical Oxygen Demand (BOD), Total dissolved oxygen (TDS) and Total suspended solids (TSS) by dilution method or standard method, 2540D and 2540C respectively as given in the Annual Book of Standard Methods for Examination of Water and Wastewater. Chemical Oxygen Demand (COD) was measured by closed reflux method (D1252-95, ASTM 1995) [7, 8]. The characterization of Leather tannery effluent is shown in Table 1.

Table 1. Characterization of leather tannery effluent.

Parameter	Quantity (mg/L)	Environmental quality standards EPA Pakistan limit (mg/L)
TDS	8450	3500
TSS	1370	400
pH	6.9	6.5-8.5
Chemical Oxygen Demand (COD)	941	400
chromium	120	1
lead	20	0.5
Sulphate	220.1	1000

2.2. Experimental assembly of rotating disk mesh electrode electro-coagulation reactor

The electrocoagulation cell was constructed from acrylic material and is cylindrical in shape, with a 6.5 cm diameter and a 22.5 cm height. It can store 1 L of wastewater and Table 2 gives specific measurements of dimensions of electrocoagulation reactor. The pH of the tannery wastewater was maintained using 2% sulfuric acid (H_2SO_4) solution and 5% sodium hydroxide solution (NaOH). The electrodes utilised were composed of iron material. After each experiment was completed, the electrodes were cleaned with diluted 2% Hydrochloric acid (HCl) solution and de-ionized water. To observe the passivation and metal oxide layer on surface of electrode SEM and EDX was used. They were then dried at 105 ˚C in an oven before being utilised for other studies. Each batch includes four plates in the electrolytic reactor acting as the anode and cathode for NRDE reactor. For RDE reactor and RDME reactor four disc electrodes were used. DC supply (TITAN TN305D) was used having range of 0-30 V and 0-5 A. After 15 min, 10 ml of the sample was removed from the electrocoagulation cell and filtered using filter paper (Whatman no. 42) to separate the effluent from the sludge in order to observe the removal performance of the electrodes [9]. By using ICP the filtrate concentration for the removal of Pb and Cr was found. To eliminate the water, the filtrate's remaining residue was dried in an oven at 105 ˚C. Detailed explanation of the electrocoagulation experimental setup can be shown in Fig. 1.

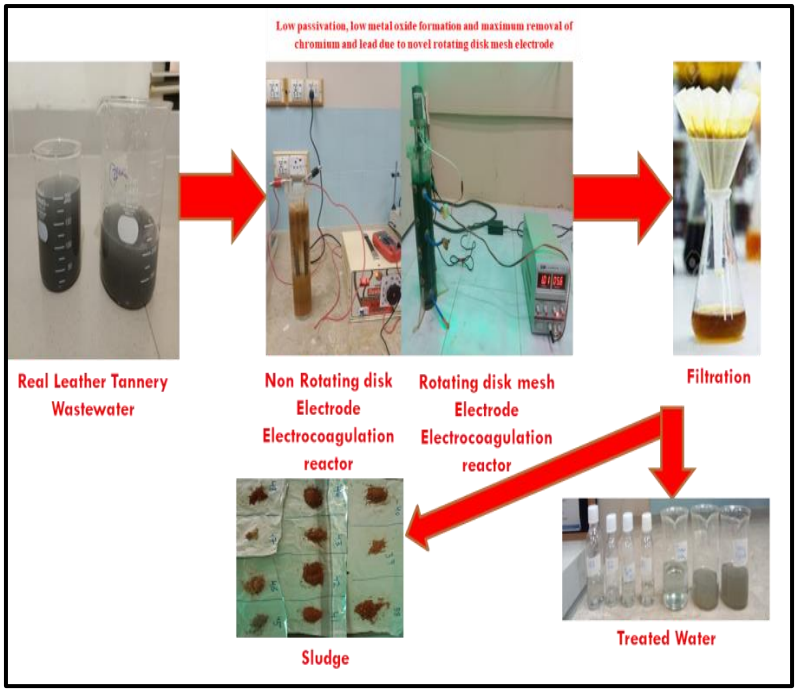

Fig. 1. Process flow diagram of experimental setup for treatment of leather tannery effluent.

The removal efficiency, specific energy consumption and energy consumption of chromium and lead was determined by Eqs. (1) to (3) respectively [10]

$$Removal\ efficiency\ (\%) = \frac{C_o - C_t}{C_o} \times 100 \quad (1)$$

$$\text{Specific energy consumption}(\text{kWh kg}^{-1}\text{m}^{-3}) = \frac{\text{VIt}}{(\text{C}_\text{o} - \text{C}_\text{t}).\ \text{v}} \quad (2)$$

$$\text{Energy consumption}(\text{kWh m}^{-3}) = \frac{VIt}{v} \quad (3)$$

where C_o (mg/L) represents concentration of pollutant before electrocoagulation and C_t (mg/L) is concentration of pollutant after electrocoagulation, V (V) is voltage and I (A) is current, v (m^3) is volume of wastewater treated and t (h) is treatment time.

Table 2. Dimensions of electrocoagulation reactor.

Electrodes	
Material (anode and cathode)	Iron
Shape	Circular (rotating disk and mesh electrodes) and rectangular (for non-rotating)
Diameter of disk anode electrode	3.2 cm
Size of nonrotating electrode	9.5 cm × 0.6 cm × 0.4 cm
Plate arrangement	Parallel
Effective one electrode Surface area rectangular and disk	19 cm^2
Thickness of anode electrode	3 mm
Diameter of ring cathode	6.4 cm
Thickness of ring cathode	1mm

Number of anode electrodes	4
Number of cathode electrode	4
Total Effective surface area	76 cm^2
Reactor characteristics	
Material	Acrylic
Shape	Cylindrical
Reactor Type	Batch Mode
Dimension	22.5 cm height and 6.5 cm diameter
Volume	1 L
Electrode gap	5 cm
Power supply	DC
Voltage	0-30 V
Current	0-5 A

2.3. Adsorption Isotherm and kinetic study

The cathode electrode releases hydroxide ions, which are combined with metal ions produced by the anode electrode during the electrocoagulation process [11]. The increase in removal percentage of Cr and Pb was due to increase of mass of adsorbent by increase in current density. The adsorbent mass can be illustrated by Eq. (4).

$$m = \frac{M \times i \times t_{EC}}{z \times F} \tag{4}$$

where M is molecular mass of iron (55.8 g/mol), i is current in amperes (A), t_{EC} is electrocoagulation time (seconds), z is number of electron transferred (z=2) and F is faraday's constant (96,487 C/mol).

The amount of Cr and Pb adsorbed onto adsorbents was determined from Eq. (5)

$$q_e = (C_o - C_e) \times v/m \tag{5}$$

where q_e (mg/g) shows the amount of chromium and lead adsorbed on surface on situ produced hydroxide of mass m (g), $\boldsymbol{C_o}$ and $\boldsymbol{C_e}$ shows initial and equilibrium concentration of pollutant chromium and lead, $\boldsymbol{v}$ shows the volume (L) of treated wastewater [12].

The separation factor of equilibrium parameter, R_L, was calculated by Eq. (6)

$$R_L = \frac{1}{1+ K_L.C_o} \tag{6}$$

The separation factor or equilibrium curve R_L indicate the favourable, un favourable adsorption and linear adsorption at R_L values $0 < R_L < 1$, $R_L > 1$ and) $R_L=1$ respectively [13].

The treatment of tannery wastewater is modelled using adsorption theory, Eqs. (7) and (8) reflect two well-known adsorption isotherm models, namely Langmuir and Freundlich, which were applied in this investigation [14]

$$\frac{1}{q_e} = \frac{1}{K_L.q_m.C_e} + \frac{1}{q_m} \tag{7}$$

$$q_e = K_F \times C_e^{1/n} \tag{8}$$

where K_L stands for the sorption Langmuir constant related with sorption free energy and sorption of chromium and lead (L/mg), and C_e is equilibrium concentration of chromium and lead in solution (mg/litre), q_m is maximum amount of chromium and lead adsorption per unit mass of sorbent (mg/g), whereas K_F [(mg/g)/(L/mg)n, 1/n (dimensionless value 0-1) gives us information about active sites, the smaller value of 1/n tell us about the presence of heterogeneous sites and physical nature of adsorption [15, 16].

Pseudo first order, pseudo second order and intra particle diffusion is given by Eqs. (9) to (11) [13, 17, 18]

$$\ln (q_e - q_t) = ln\, q_e - K_1 t \tag{9}$$

$$\frac{t}{q_t} = \frac{1}{K_2 q_e^2} + \frac{1}{qe} \tag{10}$$

$$q_t = K_{in}\, t^{1/2} + y \tag{11}$$

where t denotes the contact time (min), q_t denotes the removal of chromium and lead at that time (mg/g), K_1 denotes the rate constant of the pseudo first order kinetic model (min^{-1}), K_2 denotes the rate constant of pseudo the second order kinetic model (g/mg.min), and q_e denotes the equilibrium adsorption capacity of ions released from the iron. Langmuir and Freundlich adsorption isotherm model was used to validate the experimental results.

3. Results and Discussion

3.1. Effect of rotating disk mesh electrode as anode on removal performance

The performance of NRDE, RDE was compared with RDME electrocoagulation reactor (operating condition of pH=7, current density=19.27 mA/cm^2, RPM=160 and material of electrode iron). The initial concentration of Cr and Pb were 120 mg/L and 20 mg/L, as given in Table. 1. The NRDE reactor decreases concentration of Cr and Pb from 120 mg/L to 71.2 mg/L and 20 mg/L to 3.1 mg/L respectively from leather tannery effluent at above mentioned operating conditions.

The RDE electrocoagulation reactor decrease concentration of Pb and Cr from 20 mg/L to 0.6 mg/L and chromium from 120 mg/L to 21.5 mg/L. The RDME decrease Cr concentration from 120 mg/L to 4.8 and Pb from 20 mg/L to 0.24 mg/L. It had been determined that removal efficiency of Cr for NRDE was 35.27 %, RDE 80.43% and RDME 96% during electrocoagulation process. The removal efficiency of Pb for NRDE was 84.5 %, RDE was 97 % and RDME was 98.8% as shown in Fig. 2. RDME has greater removal efficiency as compared with rotating disk electrode because of greater surface area of contact with pollutant in effluent.

The efficiency of NRDE electrocoagulation reactor is less compared with RDE and RDME electrocoagulation reactor because rotation of electrode will decrease the passivation film, sloughs away metal oxide layer and sludge on surface of electrode, turbulence in effluent causing to exert force on layer on surface of electrode and proper diffusion of metal ions in tannery effluent. The same reason for RDME having greater efficiency for treatment of textile wastewater using electrocoagulation was also observed by Nippatla and Philip [10].

Wang et al. [19] also observed that aqueous film on coated surface of electrode reduced by using RDME for treatment of electroplating wastewater. Since periodic

cleaning of electrode is necessary to increase removal efficiency of pollutant by electrocoagulation [20]. This action is performed by itself due to rotation of electrode during electrocoagulation.

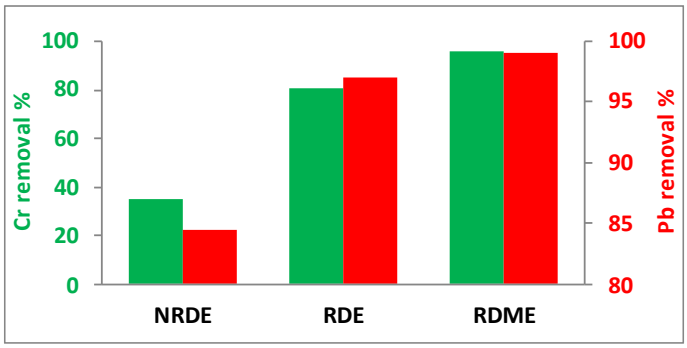

Fig. 2. Cr and Pb removal of NRDE, RDE and RDME (operating conditions pH=7, treatment time=90 min, current density= 19.27 mA/cm^2, RPM=160).

The specific energy consumption requirement for NRDE was 347.96 kWh/kg Cr and 798.81 kWh/kg of Pb, RDE was 152.58 kWh/kg of Cr and 695.87 kWh/kg Pb and RDME was 127.71 kWh/kg of Cr and 681.13 kWh/kg of Pb as shown in Fig. 3. It was deducted from results that RDME is energy efficient electrode for removing of Cr and Pb because of high removal efficiency in less time due to less metal oxide and sludge layer on surface of electrode and maximum reaction of metal ions released from electrode with Cr and Pb. Similar specific energy consumption behaviour was observed by Nippatla (2021) for treatment of textile industry waste using electrocoagulation.

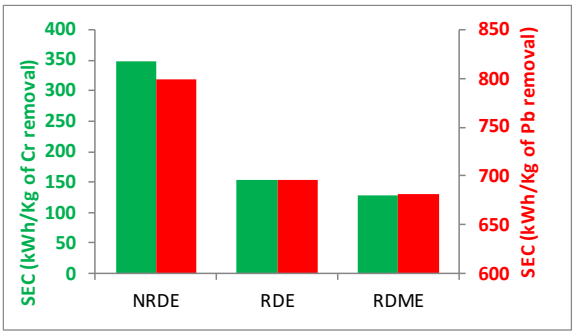

Fig. 3. Specific Energy consumption (SEC) from of NRDE, RDE and RDME (operating conditions pH=7, treatment time=90 min, current density= 19.27 mA/cm^2, RPM=160).

3.2. Physical and chemical analysis surface of electrodes

It was observed from SEM analysis there is layer of sludge and oxide fouling film on surface of all three electrodes NRDE, RDE and RDME. The metal oxide layer on surface of RDME was less as compared with NRDE and RDE as shown Fig. 4 in SEM images and similar findings were obtained from EDX as shown in Figs. 5 to 7. Figure 7 shows there is 10.45% oxygen, 1.04% Cr and 14.74 % Pb elemental

weight % after electrocoagulation experiment in case of RDME. At the same time RDE and NRDE designs shows greater weight percentages of oxygen, Cr and Pb compared with RDME design electrocoagulation process. From results of EDX it can be deducted that there is less metal oxide layer on surface of RDME design of electrocoagulation reactor than RDE and NRDE design for electrocoagulation.

Table 3. EDX analysis weight % of various elements on electrode surface.

RDME		RDE		NRDE	
Element	**Weight %**	**Element**	**Weight %**	**Element**	**Weight %**
Oxygen	10.45	Oxygen	16.81	Oxygen	17.7
Chromium	1.04	Chromium	1.21	Chromium	1.7
Lead	14.34	Lead	15.03	Lead	16.1
Sodium	12.29	Sodium	2.8	Sodium	0.8
Carbon	4.8	Carbon	5.2	Carbon	4.15
Iron	57.08	Iron	58.45	Iron	60.15
Total	**100**	**Total**	**100**	**Total**	**100**

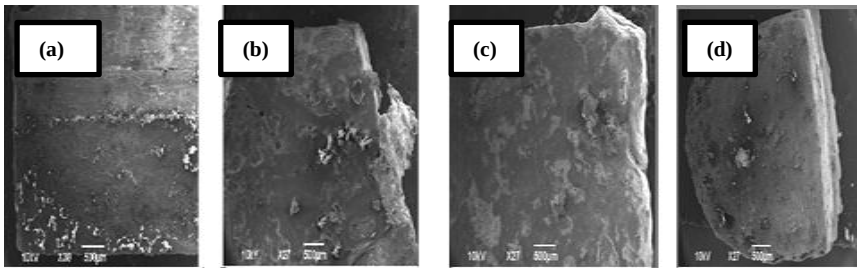

Fig. 4. SEM analysis of electrodes (a) NRDE before experiment (b) NRDE after experiment (c) RDE after experiment (d) RDME after experiment.

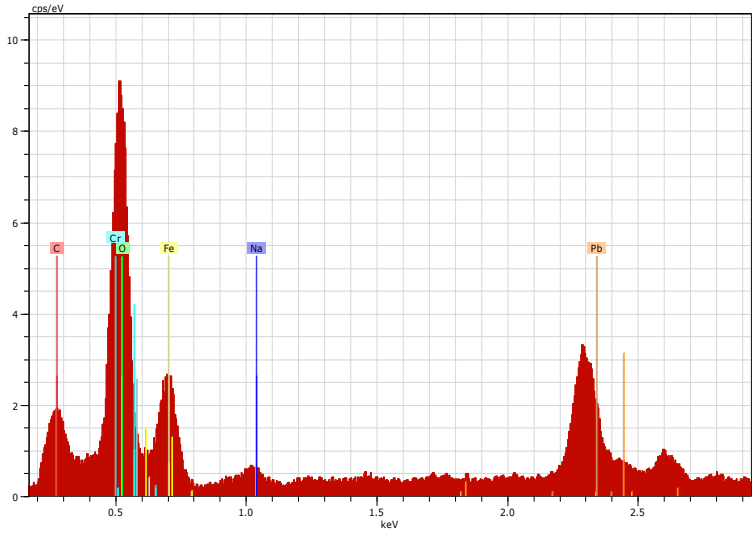

Fig. 5. EDX analysis of NRDE (operating condition pH=7, Current density=19.27 mA/cm^2, RPM=160).

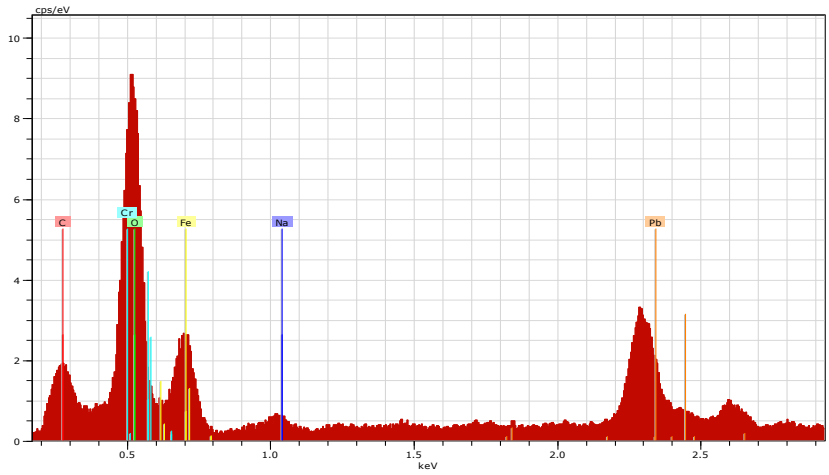

Fig. 6. EDX analysis of RDE (operating condition pH=7, Current density=19.27 mA/cm^2, RPM=160).

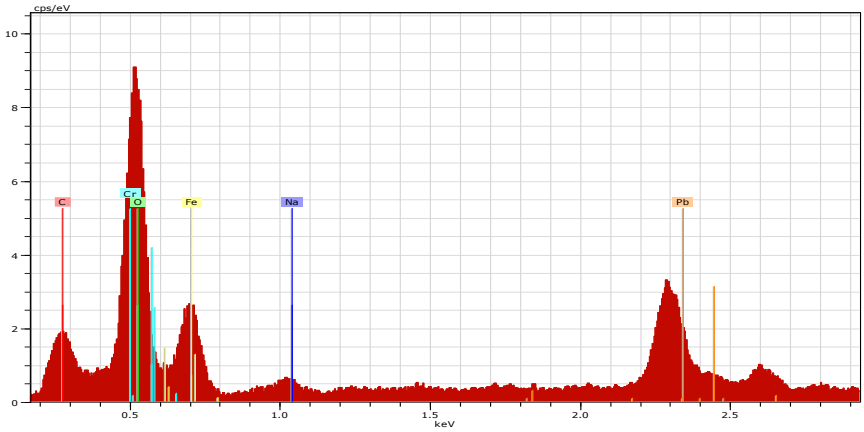

Fig. 7. EDX analysis of RDME (operating condition pH=7, Current density=19.27 mA/cm^2, RPM=160).

3.3. Effect of reaction time on removal efficiency of electrodes

From Fig. 8, it is clear that the RDME removes Cr and Pb more effectively than NRDE and RDE. Cr removal took 90 min to establish equilibrium, and Pb removal took 15 min. Pb can be eliminated earlier during the electrocoagulation process than Cr because Pb forms an insoluble iron hydroxide-complex. Compared to Cr, which exits in +3 and +6 oxidation states and requires more negatively charged metal hydroxide complex to destabilize from wastewater or has a high oxidation state and small atomic radius, the iron electrode has a stronger affinity to remove Pb in less time. Pb has a high atomic radius and +2 charge at the same time since electrocoagulation is mainly dependent on reaction of metal released in form of ions. So the Pb is removed in less time as compared with Cr. It was also observed that removal performance of chromium and lead was greater in initial 15 min than

it was decreased for Cr removal and remains constant for Pb. According to Faraday law iron dissolution increases in wastewater with time [21]. Initially the electrode has no or minimum external material on surface of electrode after that the formation of layer on surface of electrode developed causing to decrease reaction of electrode material with Cr and Pb [22].

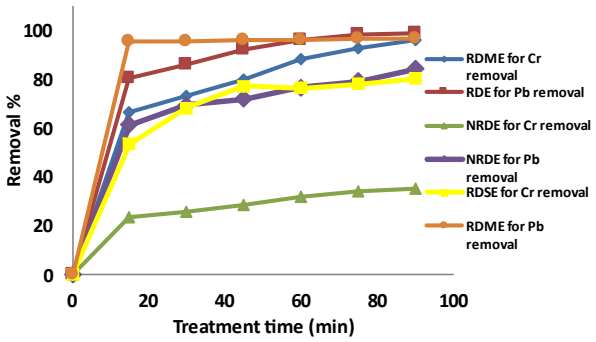

Fig. 8. Effect of treatment time of NRDE electrocoagulation reactor, RDE electrocoagulation reactor and RDME electrocoagulation reactor on Cr and Pb removal (operating conditions pH=7, current density= 19.27 mA/cm^2, RPM=160).

3.4. Comparison of previous studies with current study for treatment of leather tannery effluent

The related studies for Cr and Pb detoxification from leather tannery wastewater were compiled for removal efficiency and energy consumption requirement as shown in Table 4. It was obtained from results that rotating disk mesh electrode used in this study has appreciable removal performance of Cr=96% and Pb=98.8% simultaneously within 90 min. In addition to energy requirement is one of the main parameter for feasibility of electrocoagulation process and it was determined in this study energy consumption requirement was 24.75 kWh/m^3. Thus the results of study revealed that rotating disk mesh iron electrode used in electrocoagulation has the lowest energy consumption and maximum efficient removal of chromium and lead compared with other studies.

Table 4. Comparison of removal performance Cr and Pb with previous studies.

Initial Conc. of pollutant	Operating conditions	Pollutant removal and final concentration (mg/L)	Energy consumption (kWh/m^3)	References
Cr=50 mg/L, Pb=20 mg/L, pH=6.5,Conductivity=2.4 mS/cm	Electrode material Aluminium, Volume of wastewater handled 1.4 dm^3, DC supply 0-30 volts, 0-5 A, RPM=180, treatment time=90 min and surface area=272 cm^2	Cr=55.2%, Pb=58.3% & Cr=22.4 , Pb=8.34	24.96	[23]

Cr=30 mg/L	Electrode material Aluminum , pH 3, current density 40 mA/cm^2, Treatment time =30 minutes, capacity of reactor 0.7 L, surface area 60 cm^2	Cr=84.2% and Cr=4.8	30	[24]
Cr=7000 mg/L	Electrode material Aluminium plate electrode, Current density 400A/m^2, 6 h, surface area =210 cm^2	Cr=87% and Cr=910	35	[25]
Cr=120 mg/L Pb=20 mg/L	Electrode material Iron, RDME, surface area 76 cm^2, treatment time=90 min, current density=26.7 mA/cm^2,initial pH=7, RPM=160	Cr=96 %, Pb=98.8%, Cr=4.8 Pb=0.24	24.75	This study

3.5. Isotherm modelling study of rotating disk mesh electrocoagulation (RDME) reactor

Electrocoagulation study was performed at fixed initial concentration of Cr and Pb at known current densities amount of adsorbent dose was determined by Eq. (5). It was observed from experiment that increases in adsorbent mass increases the removal percentage of Cr and Pb as shown in Fig. 9.

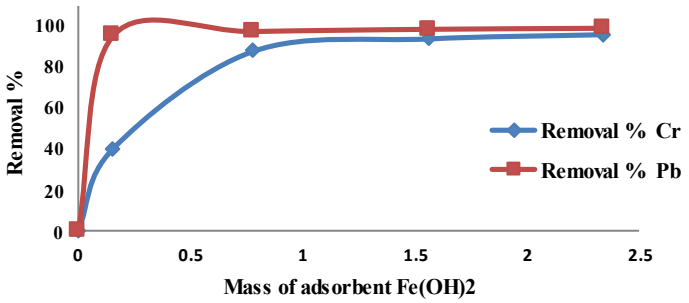

Fig. 9. Removal % of Cr and Pb by rotating disk mesh electrode design v/s mass of adsorbent (operating condition current density 26.57 mA/cm^2, RPM=160, treatment time=90 min, initial concentration of Cr=110 mg/L & Pb=20 mg/L).

The ability to anticipate and compare experimental and modelled adsorption capacities, as well as to design the total adsorption ability of ferrous ions produced from electrodes in the electrocoagulation process, is achieved through the application of the adsorption isotherm models technique [14, 26, 27]. The Langmuir isotherm told us about mechanism of monolayer adsorbate deposition on generated hydroxide (coagulant/adsorbents) [28]. The equilibrium parameters q_m and K_L can be calculated by slope and intercept of linear plot between $1/q_e$ against

1/Ce as illustrated by Eq. (6) [29]. The batch experimental data suit the popular Langmuir and Freundlich isotherm models given by Eq. (7) and shown in Fig. 10(a) to 10(d).

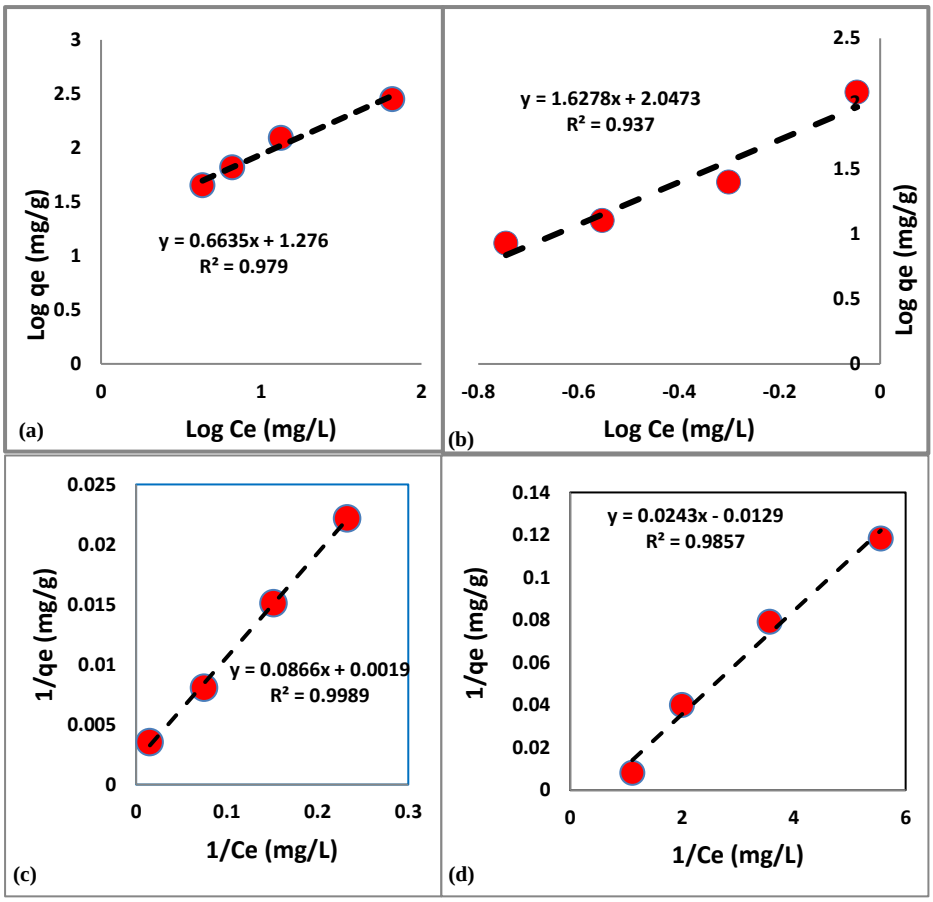

Fig. 10(a). Freundlich adsorption isotherm for Cr (b) Freundlich adsorption isotherm for Pb (c) Langmuir adsorption isotherm for Cr (d) Langmuir adsorption isotherm for Pb.

for the adsorption isotherm of Cr and Pb by iron material RDME. Table 5 both Langmuir and Freundlich model parameters are shown K_L (Langmuir constant), 1/n (dimensionless value), R_L, q_m (maximum adsorption capacity) and K_f (Freundlich constant). From the experimental data we determined that R^2 value of Langmuir isotherm model was greater than Freundlich adsorption isotherm for chromium and lead. Besides this, the experimental adsorption capacity was (q_{exp}= 283.5 mg/g) was very close Langmuir model calculated adsorption capacity ($q_{eLangmuir}$=310 mg/g) for Cr. From results it was deducted that R_L=0.292 for Cr and 0.842 for Pb favourable adsorption occur during electrocoagulation process. Though Langmuir closely resembles for Cr and Pb removal from Tannery effluent. The Langmuir model was also proved to be appropriate for iron electrodes for removal of Cr and Pb from tannery effluent.

Table. 5 Adsorption isotherm model parameter value for Cr and Pb removal by Electrocoagulation.

	Parameters							
Isotherm model	**q_m (mg/g) for Cr**	**K_L for Cr** (L/mg)	**R^2**	**R_L**	**q_m for Pb (mg/g)**	**K_L for Pb** (L/mg)	**R^2**	**R_L**
Langmuir	526.31 mg/g	0.021	0.99	0.29	5000	0.00935	0.985	0.84
Freundlich	**K_f for Cr**(mg/g)/(L/mg)	**1/n for Cr**	**R^2**		**K_f for Pb** (mg/g)/(L/mg)	**1/n for Pb**	**R^2**	
	18.87	0.66	0.979		97.72	1.53	0.937	

3.6. Kinetic study for removal of chromium and lead

There were a lot of initial large vacant sites on the adsorbent surface, a rapid rate of adsorption was observed in the first 15 min of reaction time. Following that a noticeable decline in adsorption rate was seen after 90 min of contact time, equilibrium was attained. Due to the repulsive forces between Cr and Pb on the surface and in solution, remaining vacant sites on the adsorbent surface are too complicated to be filled once equilibrium has been attained. Pb and Cr can no longer be absorbed in this way [30, 31]. In order to better understand the kinetic behaviour of Cr and Pb removal by ferrous ion as generated by electrocoagulation, experimental data was modelled through pseudo first order as shown in Figs. 11(a) to 11(d), pseudo second order as shown in Figs. 12(a) to 12(d) and intra particle diffusion model as shown in Figs. 13(a) to 13(d). The electrocoagulation experiment's results that intra particle diffusion model explains and validates the sorption process's mechanism. This procedure may involve two or more successive steps which are as follows: (1) Film or surface diffusion (2) adsorbate molecules moved into the interior of adsorbent particles through intra-particle or pore diffusion (3) Adsorption occurred on the interior sites of the adsorbent [12, 32], C is the intercept and k_{id} is the intra particle diffusion rate (mg/gm.min$^{1/2}$).

The values of experimental and calculated q_e with R^2 and kinetic model constants are presented in Table 6. It can be seen that the pseudo second order kinetic model's estimated and experimental q_e values are adequate with R^2 values of 0.99 for the elimination of Cr and 1 for Pb removal respectively. Hence pseudo second order kinetic model was suitable for adsorption by electrocoagulation for removal of Cr and Pb. The value of rate constant K_2= 0.00548 g/mg.min for Cr and K_2=0.0864 g/mg.min for Cr, it indicates that rate of second order rate constant was greater for Pb shows the adsorption at greater rate. It was determined that 90 minutes was suitable contact time after that adsorption reached equilibrium. Figures 13(a) and 13(b) show the plot of q_t versus $t^{1/2}$ for Cr removal and q_t versus $t^{1/2}$ for Pb removal in Figs. 13(c) and 13(d) show experimental and calculated q_t values correlation by fitting experimental data in to intra particle diffusion model. The plots presented was linear line with R^2= 0.992 and 0.9597 for Cr and Pb respectively. Figures 11(a) and 11(b) suggest that diffusion of Cr and Pb on surface of adsorption was rate limiting step. However, the fact that the linear lines in both cases did not pass through the origin demonstrates that the rates of Cr and Pb uptake during the initial and end stages differ, indicating that adsorption is constrained by additional kinetic models that might be active at the same time [29]. Additionally, the thickness of the boundary layer between the adsorbate-adsorbent interfaces is

estimated by the value of the diffusion layer boundary, which is determined to be 53.81 mg/g for Cr and 24.27 mg/g for Pb, respectively.

The rate constant K_{id} value was found to be equal to 7.47 and 0.0688 for Cr and Pb respectively. The larger the intercept the greater is the boundary layer effect and the slower the rate [33].The larger value of Cr shows higher boundary layer effect and low rate than lead and it was also shown from experimental results. From the experimental results it was determined that 0.9>Ri>0.5 and 0.1< C/q_{ref}<0.5 initial adsorption was in the intermediate stage [32], i.e., zone 2 for Cr removal and for Pb removal is in complete initial adsorption, i.e., zone 4.

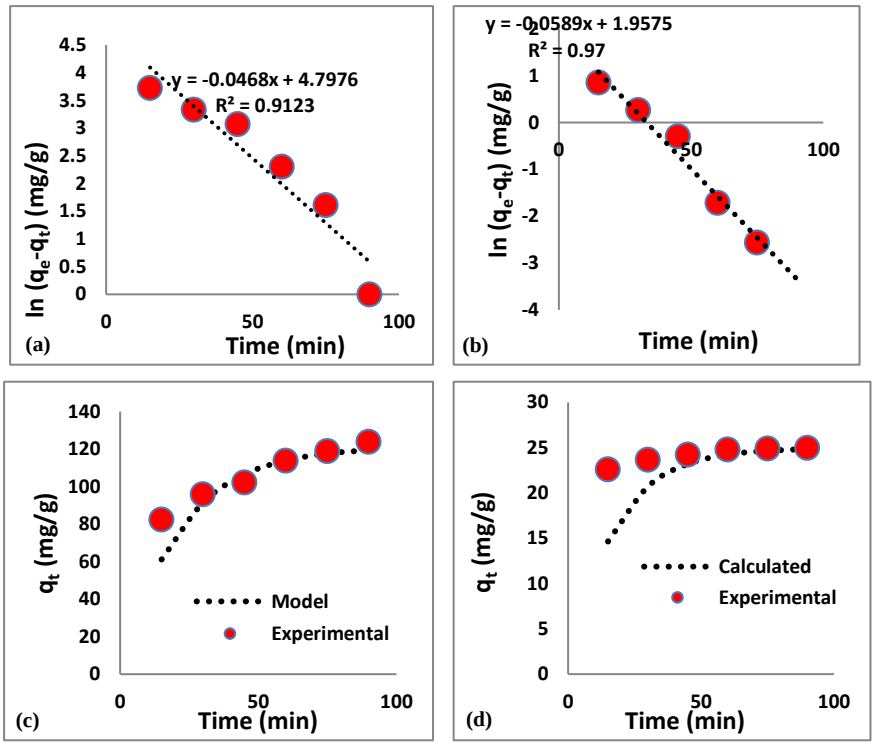

Fig. 11(a). Pseudo First order kinetic model for Cr removal (b) Pseudo First order kinetic model for Pb (c) Pseudo First order kinetic model fitted to experimental data of Cr removal (d) Pseudo second order kinetic model fitted to experimental data of Pb removal.

Table 6. Adsorption kinetic model constants of Cr and Pb removal by electrocoagulation.

	Kinetic models						
	Pseudo-first order kinetic model				Pseudo-second order kinetic model		
Parameters	**Exp. q_e (mg/g)**	**Cal. q_e (mg/g)**	**K_1(min^{-1})**	**R^2**	**Cal. q_e (mg/g)**	**K_2 (g/mg.min)**	**R^2**
Cr removal	123.76	119.42	0.046	0.91	121.7	0.000581	0.994
Pb removal	24.95	24.65	0.058	0.97	24.95	0.088	0.999

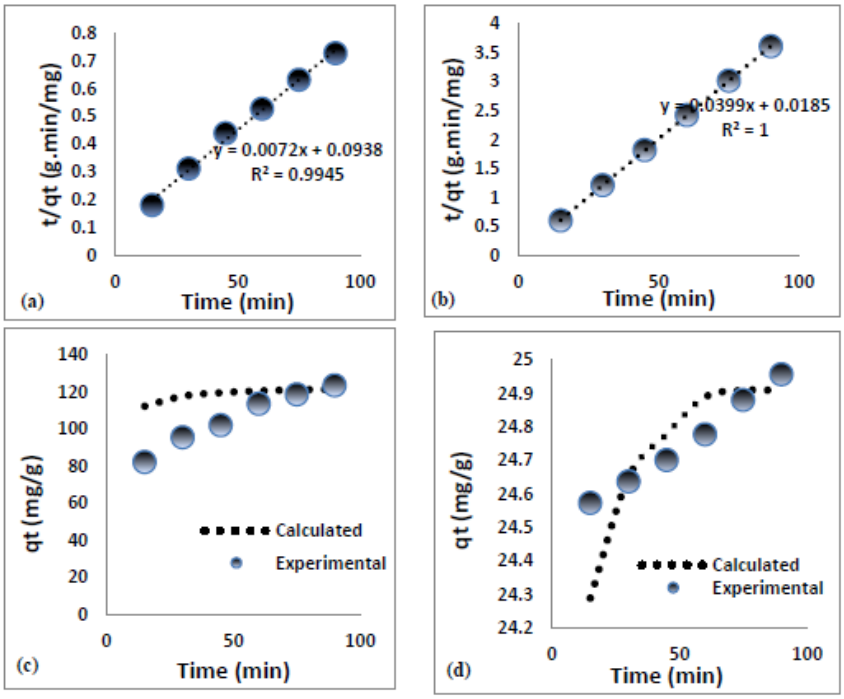

Fig. 12(a). Pseudo second order kinetic model for Cr removal (b) Pseudo second order kinetic model for Pb removal (c) Pseudo second order kinetic model fitted to experimental data for Cr removal (d) Pseudo second order kinetic model fitted to experimental data for Pb removal.

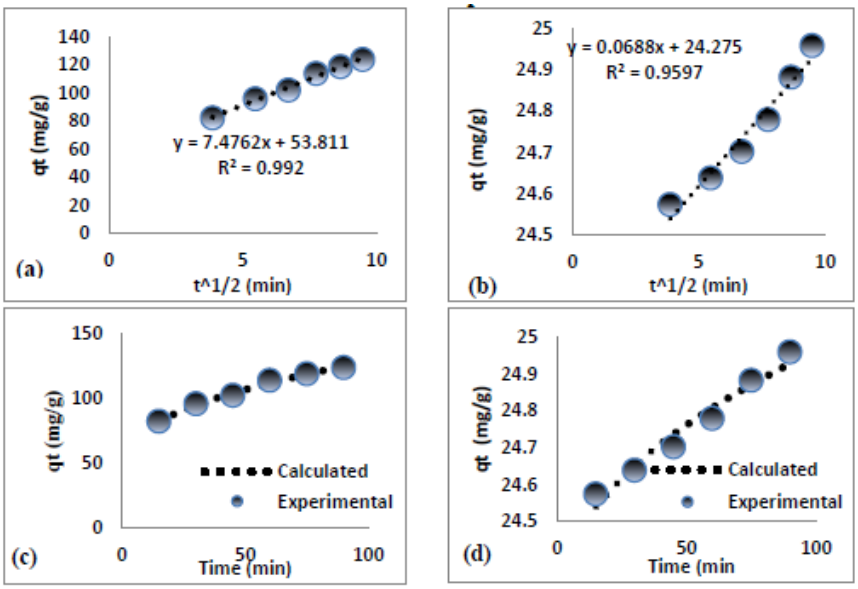

Fig. 13. (a) Intra particle diffusion model for Cr removal (b) Intra particle diffusion model for Pb removal(c) Intra particle diffusion model fitted to experimental for Cr removal (d) Intra particle diffusion fitted to experimental data for Pb removal.

4. Conclusion

The passivation, metal oxide layer on surface of NRDE, RDE and RDME of iron material was examined at pH=7, current density=19.57 mA/cm^2, RPM=160 and treatment time=90 min. It was determined from this study that RDME has less passivation on electrode surface and maximum removal efficiency of Cr 96 % and Pb 98.8% than other design of electrodes used in electrocoagulation process. This result revealed that RDME is best electrode design for use in electrocoagulation of leather tannery effluent at large scale application because of less passivation on surface of electrode, less energy consumption and environment friendly than conventional electrode design used in electrocoagulation process. It was calculated using the correlation coefficient R^2 for Cr and Pb, which had values of 0.999 and 0.98, respectively and was well fitted with experimental data using the Langmuir model. It demonstrates the mechanism of monolayer adsorption during electrocoagulation on adsorbent produced from RDME. It was discovered that experimental values have good agreement with the pseudo second order kinetic model and Langmuir adsorption isotherm models.

Acknowledgement

Author is thankful to Advanced Material and Membrane Technology Laboratory Technical University of Denmark and Chemical Engineering Department Mehran University of Engineering and Technology Jamshoro Sindh Pakistan.

Nomenclatures

C	Boundary layer thickness
C_o	Initial concentration of pollutant, mg/l
Cr	Chromium
C_t	Final concentration of pollutant, mg/l
I	Current, Amp
K_1	First order rate constant, min-1
K_2	Second order rate constant, g/mg.min
K_F	Freundlich constant, (mg/g)/(L/mg)
K_{id}	Intra particle diffusion model rate constant
K_L	Langmuir constant, (L/mg)
m	Adsorbent mass, g
Pb	Lead
q_e	Equilibrium adsorption capacity mg/gm
q_m	Maximum adsorption capacity, mg/gm
q_{ref}	solid phase concentration at time (t)=tref
q_t	Adsorption capacity at any time t, mg/gm
R_2	Correlation coefficient
R_i	Initial adsorption factor
R_L	Separation factor
t	Treatment time, h
v	Volume of wastewater treated, m^3 and L

Abbreviations

ASTM	American Society for testing materials

EDX	energy dispersive X-Ray Spectrometry
ICP	Inductively coupled plasma
NRDE	Non-Rotating Disk Electrode
RDE	Rotating Disk Electrode
RDME	Rotating Disk Mesh Electrode
SEM	Scanning electron microscopy

References

1. Murtaza, G.; and Usman, M. (2022). Assessment of various heavy metals level in groundwater and soil at tannery manufacturing areas of three mega cities (Sialkot, Lahore and Karachi) of Pakistan. *Desalination and Water Treatment*, 266, 121-130.
2. Song, Z.; Williams, C.; and Edyvean, R. (2004). Treatment of tannery wastewater by chemical coagulation. *Desalination*, 164(3), 249-259.
3. Ouaissa, Y.A.; Chabani, M.; Amrane, A.; and Bensmaili, A. (2012). Integration of electro coagulation and adsorption for the treatment of tannery wastewater-The case of an Algerian factory, Rouiba. *Procedia Engineering*, 33, 98-101.
4. Keerthi; Suganthi, V.; Mahalakshmi, M.; and Balasubramanian, B. (2013). Development of hybrid membrane bioreactor for tannery effluent treatment. *Desalination*, 309, 231-236.
5. Deghles, A.; and Kurt, U. (2016). Treatment of tannery wastewater by a hybrid electrocoagulation/electrodialysis process. *Chemical Engineering and Processing: Process Intensification*, 104, 43-50.
6. Garcia-Segura S.; Eib, M.M.S.G.; de Melo, J.V.; and Martínez-Huitle, C.A. (2017). Electrocoagulation and advanced electrocoagulation processes: A general review about the fundamentals, emerging applications and its association with other technologies. *Journal of Electroanalytical Chemistry*, 801, 267-299.
7. ASTM. (1995). *Standard test methods for chemical oxygen demand* (*dichromate oxygen demand*) *of water*. Annual Book of ASTM Standards, D1252-95.
8. Eaton, A.D., Clesceri, L.S.; Greenberg, A.E.; and Franson, M.A.H. (1995). *Standard methods for the examination of water and wastewater*. American Public Health Association, Washington, DC, USA.
9. Sharma, D.; Chaudhari, P.K.; and Prajapati, A.K. (2020). Removal of chromium (VI) and lead from electroplating effluent using electrocoagulation. *Separation Science and Technology*, 55(2), 321-331.
10. Nippatla, N.; and Philip, L. (2020). Performance evaluation of a novel electrolytic reactor with rotating and non rotating bipolar disc electrodes for synthetic textile wastewater treatment. *Journal of Environmental Chemical Engineering*, 8(2), 103462.
11. Ghahrchi, M., Rezaee, A., and Adibzadeh, A. (2021). Study of kinetic models of olive oil mill wastewater treatment using electrocoagulation process. *Desalination Water Treatment*, 211, 123-130.
12. Alothman, Z.A.; Naushad, M.; and Ali, R. (2013). Kinetic, equilibrium isotherm and thermodynamic studies of Cr (VI) adsorption onto low-cost

adsorbent developed from peanut shell activated with phosphoric acid. *Environmental Science and Pollution Research*, 20, 3351-3365.

13. Zarrabi, M.; Soori, M.M.; Sepehr, M.N.; Amrane, A.; Borji, S.; and Ghaffari, H.R. (2014). Removal of phosphorus by ion-exchange resins: equilibrium, kinetic and thermodynamic studies. *Environmental Engineering & Management Journal*, 13(4), 891.
14. Chen, X. (2015). Modeling of experimental adsorption isotherm data. *Information*, 6(1), 14-22.
15. Malhotra, M.; Suresh, S.; and Garg, A. (2018). Tea waste derived activated carbon for the adsorption of sodium diclofenac from wastewater: adsorbent characteristics, adsorption isotherms, kinetics, and thermodynamics. *Environmental Science and Pollution Research*, 25, 32210-32220.
16. Cao, J.-S.; Lin, J.-X.; Fang, F.; Zhang, M.-T.; and Hu, Z.-R. (2014). A new absorbent by modifying walnut shell for the removal of anionic dye: kinetic and thermodynamic studies. *Bioresouce Technology*, 163,199-205.
17. Aoudj, S.; Khelifa, A.; Drouiche, N.; Belkada, R.; and Miroud, D. (2015). Simultaneous removal of chromium (VI) and fluoride by electrocoagulation-electroflotation: application of a hybrid Fe-Al anode. *Chemical Engineering Journal*, 267, 153-162.
18. Moussout, H.; Ahlafi, H.; Aazza, M.; and Maghat, H. (2018). Critical of linear and nonlinear equations of pseudo-first order and pseudo-second order kinetic models. *Karbala International Journal of Modern Science*, 4(2), 244-254.
19. Wang, J.; Chen, X.; Yao, J.; and Huang, G. (2015). Decomplexation of electroplatingwastewater in a higee electrochemical reactor with rotating mesh-disc electrodes. *International Journal of Electrochemical Science*, 10(7), 5726-5736.
20. Chen, G. (2004). Electrochemical technologies in wastewater treatment. *Separation and Purification Technology*, 38(1), 11-41.
21. Kobya, M.; Demirbas, E.; and Ulu, F. (2016). Evaluation of operating parameters with respect to charge loading on the removal efficiency of arsenic from potable water by electrocoagulation. *Journal of Environmental Chemical Engineering*, 4(2), 1484-1494.
22. Kobya, M.; Gebologlu, U.; Ulu, F.; Oncel, S.; and Demirbas, E. (2011). Removal of arsenic from drinking water by the electrocoagulation using Fe and Al electrodes. *Electrochimica Acta*, 56(14), 5060-5070.
23. Sharma, D.; Pal, D.; Athankar, K.K., Prajapati, A.K.; and Mehra, S. (2023) Removal of chromium (VI) and lead from synthetic solution using electrocoagulation: optimization and performance study. *Brazilian Journal of Chemical Engineering*, 1-11.
24. Tibebe, D.; Asmare, M.; and Mulugeta, M. (2021). Treatment and characterization of chromium from tannery industry effluents by electrocoagulation process using aluminum electrode. *Ethiopian Journal of Natural and Computational Sciences*, 1(1), 79-89.
25. Elabbas, S.; Ouazzani, N.; Mandi, L.; Berrekhis, F.; Perdicakis, M.; Pontvianne, S.; Pons, M.-N.; Lapicque, F.; and Leclerc, J.-P. (2016). Treatment of highly concentrated tannery wastewater using electrocoagulation: influence

of the quality of aluminium used for the electrode. *Journal of Hazardous Materials*, 319, 69-77.

26. Nimibofa, A.; Ebelegi, A.N.; and Donbebe, W. (2017). Modelling and interpretation of adsorption isotherms. *Journal of Chemistry*, Volume 2017, Article ID 303981.
27. Li, W.; Zheng, P.; Guo, J.; Ji, J.; Zhang, M.; Zhang, Z.; Zhan, E.; and Abbas, G. (2014). Characteristics of self-alkalization in high-rate denitrifying automatic circulation (DAC) reactor fed with methanol and sodium acetate. *Bioresource Technology*, 154, 44-50.
28. Dai, Y.; Niu, J.; Yin, L.; Xu, J.; and Xi, Y. (2011). Sorption of polycyclic aromatic hydrocarbons on electrospun nanofibrous membranes: sorption kinetics and mechanism. *Journal of Hazardous Materials*, 192(3), 1409-1417.
29. Nyangi, M.J.; Chebude, Y.; Kilulya, K.F.; and Salim, C.J. (2021). Comparative study on adsorption isotherm and kinetics of defluoridation using aluminum and iron electrodes in electrocoagulation. *Chemistry Africa*, 4, 391-398.
30. Erto, A.; Natale, F.D.; Musmarra, D.; and Lancia, A. (2015). Modeling of single and competitive adsorption of cadmium and zinc onto activated carbon. *Adsorption*, 21, 611-621.
31. Yu, L.J.; Shukla, S.S.; Dorris, K.L.; Shukla, A.; and Margrave, J.L. (2003). Adsorption of chromium from aqueous solutions by maple sawdust. *Journal of Hazardous Materials*, 100(1-3), 53-63.
32. Pholosi, A.; Naidoo, E.B.; and Ofomaja, A.E. (2020). Intraparticle diffusion of Cr (VI) through biomass and magnetite coated biomass: A comparative kinetic and diffusion study. *South African Journal of Chemical Engineering*, 32, 39-55.
33. Lattanzi, A.M.; Pecha, M.B.; and Bharadwaj, V.S.; Ciesielski P.N. (2020). Beyond the effectiveness factor: Multi-step reactions with intraparticle diffusion limitations. *Chemical Engineering Journal*, 380, 122507.